Ballistic Flight Phase Simulation with euces Tool for ESC-A Upper Stage

Armin Isselhorst, Functional Propulsion Engineering, TE59
EADS Astrium GmbH, P.O. Box 286156, 28361 Bremen, Germany

Kai Bergemann, Commercial Programs, TP431
EADS Astrium GmbH, 81663 München, Germany

euces was initiated for the increased future propulsion system analysis demands. It is specifically dedicated to the development of new stage propulsion system analysis software for the simulation of functional behaviour of launcher stages during its ground and flight phases. The paper will present for euces stage simulation capability a brief overview of the various COMPONENT libraries involved and an application example which will be a simplified functional model of the ARIANE 5 ESC-A (Étage Superieur Cryotechnique) upper stage in ballistic flight configuration. The simulation results will be compared to respective flight measurement data of an ARIANE 5 upper stage ESC-A.

Nomenclature

β	=	volume expansivity
C	=	capacitance
c_p	=	specific heat capacity
γ	=	isochoric tension coefficient
η	=	dynamic viscosity
h	=	specific enthalpy
κ	=	isothermal compressibility
λ	=	heat conductivity
p_s	=	saturation pressure
R	=	resistance
ρ	=	density
T_s	=	saturation temperature
σ	=	surface tension
u	=	specific internal energy
Z	=	compressibility factor for state equation

I. Introduction

THE euces S/W development is an EADS Astrium *internal initiative* specifically dedicated to the development of launcher system and stage analysis software for the simulation of functional behaviour of launcher stages during its ground and flight phases. It incorporates the time-dependent simulation of the complete propulsion system including all its interacting components. In more detail, it comprises the evaluation of pressurant and propellant consumption, mass flows in the piping system, pressure regulation, feed-line chill-down in case of cryogenic propellants, engine characteristic parameters, ignitions and shut-down of engine and the sequence evaluation for the main propulsion or attitude control system. The categories involved are heat and mass transfer, thermodynamics, hydraulics, pneumatics, phase change of propellants, combustion, control and thermal aspects, as well as specific component design for tanks, valves, regulators, turbo machinery and rocket engines as a central role.

For the relevant hardware component formulation the existing hardware design of Ariane 5 upper stages was taken into consideration i.e. all hardware components have to be mathematically modelled adequately having an impact on the system simulation results.

euces is based on EcosimPro kernel which was initially an ESA funded S/W tool developed by EAI for dynamic modelling and simulation for networks incorporating fluid flow (gaseous and liquid), heat and mass transfer, chemical reactions, controls, etc) providing a user-friendly simulation environment for modelling simple and complex physical processes. It provides an object-oriented approach towards creating reusable component libraries and expresses the system behaviour in terms of differential-algebraic equations and discrete events. It allows creating schematic models incl. data initialization of the components and generates variable outputs, graphical charts, variable lists. The COMPONENTs will be linked via PORTs together to a complete system. PORTs are needed to exchange interconnection information between COMPONENTs as e.g. pressure, temperature or mass flow rate.

II. Component Library Development

The objective of the euces project is the development of object-oriented S/W using EcosimPro kernel for functional physical model formulations and simulation of space propulsion H/W components and systems. The project tasks are linked to:

- tanks of known geometric configuration under 1g liquid level position
- pneumatic pipe system elements
- hydraulic pipe system elements
- control system elements
- engine system elements
- agglomeration in Libraries
- generation of simulation models of dedicated sub-systems
- generation of simulation models of dedicated propulsion systems
- comparison to ground/flight measurements

The actual components for ballistic flight phase model of the cryogenic stage ESC-A in "workspace" euces are briefly presented from the different libraries.

AUXILLARY:

- global constants, complementary CONTROL (EAI) components, port definitions, complementary mathematical functions

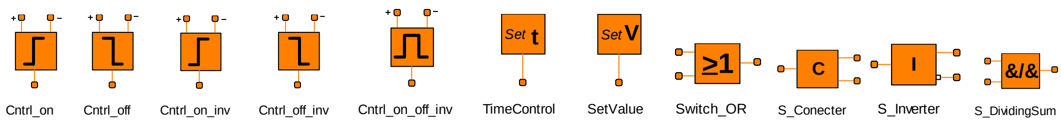

Mathematical functions have been implemented for solving quadratic and cubic equation, for linear curve and plane interpolation, for calculation of grid cover matrixes for static and moving grids.

SOLID_PROPERTIES:

- Titan, Carbon, AL2219, H920A, Dacron filled with He, Dacron filled with N_2, Cryosof, AL7020, stainless steel, copper, nickel

The solid properties considered are density ρ, heat conductivity λ, specific heat capacity c partly in dependence of temperature T.

FLUID_PROPERTIES:

- Air, H_2, He, MMH, N_2H_4, N_2, N_2O_4, O_2, H_2O, R123, HFE7000

The fluid properties considered are for *ideal* gas and liquid phase density ρ, saturation pressure p_s, saturation temperature T_s, specific isobaric/isochoric heat capacity c_p/c_v, specific enthalpy h, specific internal energy u, isothermal compressibility κ, volume expansivity β, isochoric tension coefficient γ, heat conductivity λ, dynamic viscosity η, surface tension σ. In case of He also a real gas factor Z is considered as well as a pressure dependence for the specific enthalpy h.

GAS_TANKS_1D:

- gas part: 1 gas, 1D discretized, 2 gas in PORT
- spherical tank wall: heat conduction 2D discretized
- internal heat transfer functions

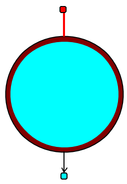

TANK_SPHERE_Gas

PROP_TANKS_1D:

- ullage part: 2 gasses, 2 gas in PORT
- liquid part: 1D pure liquid or 0D 2-phase
- moving liquid level with surface calculation
- internal heat and mass transfer functions
- different tank shapes
- tank wall 2D heat conduction
- time-dependent external heat load tables in dependence of surface temperature for convection/radiation

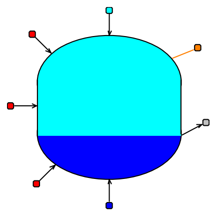

RESO_TANK

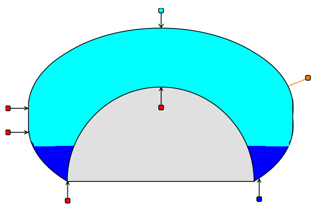

RESOU_TANK

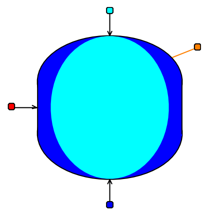

RESO_TANK_SPIN

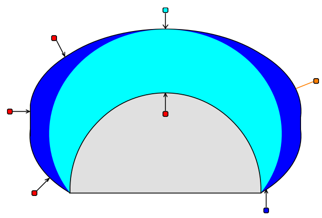

RESOU_TANK_SPIN

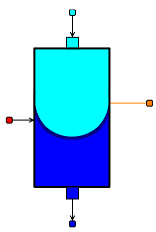

REC_TANK_0G

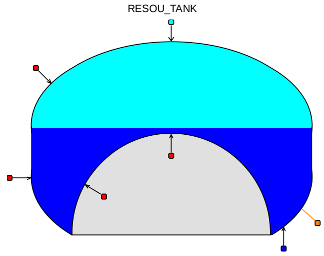

RESOUB_TANK

PNEUMATIK_2G

- gas components: 2 gasses, 2 gas in PORT, forward/backward flow
- pipes (RC) and volumes (C) include gas volume with thermodynamic properties and consideration of wall and loss calculation
- divider/combiner (RC) include gas volume with thermodynamic properties and flow calculation
- valves, orifice, filter (R) consider flow calculation

- check valves, regulators (R) consider dynamic force balance at poppet and flow calculation in dependence of poppet position
- cold gas thruster (R) consider flow calculation, performance is modelled via nozzle equation

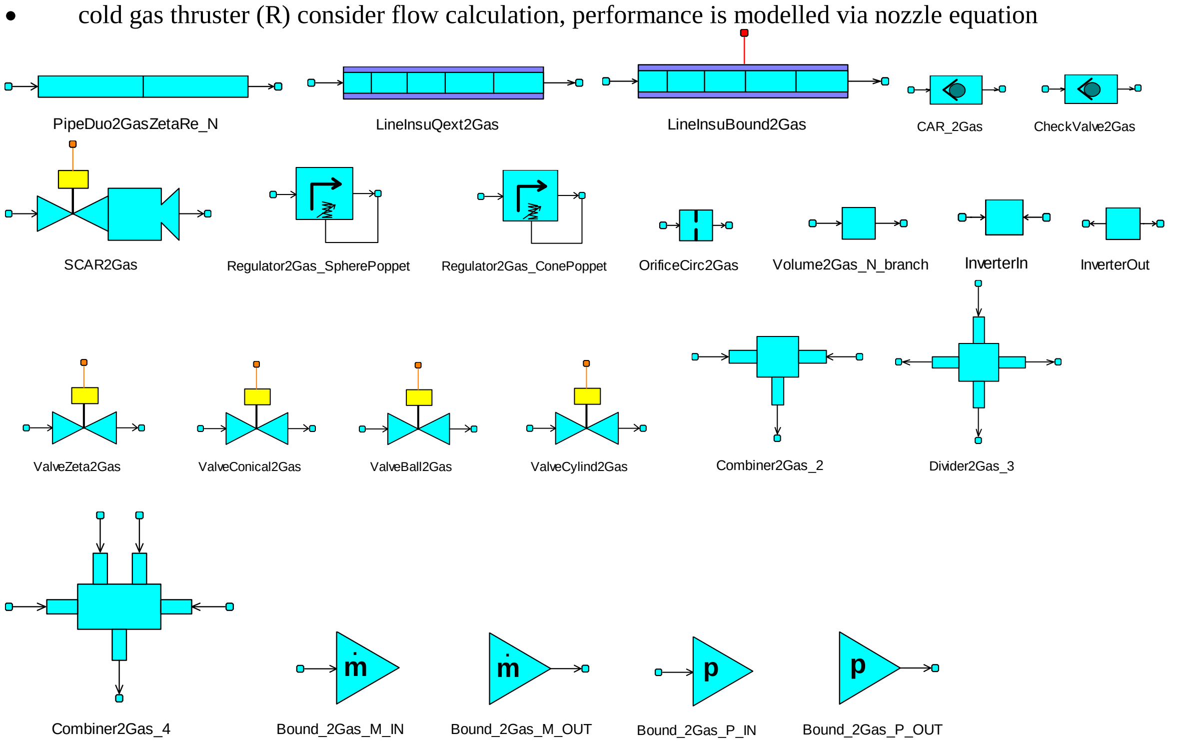

III. The ARIANE 5 ESC-A Upper Stage

The bi-propellant cryogenic upper stage Étage Supérieur Cryotechnique A (ESC-A) is the latest improvement of the ARIANE 5 and can be used instead of the EPS in case re-ignition is *not* needed. Being the 3rd and last stage ESC-A completes the mission by ejecting satellite into their specified orbit. It is the main contribution to the ability of lifting up to 9 t into GTO. The ESC-A has a reference diameter of 5400 mm and a height of 4711.6 mm (outer covering). The two propellant tanks for liquid Hydrogen and liquid Oxygen have a volume of 39.4 m^3 and 11.4 m^3, respectively. The Liquid Hydrogen (LH2) tank is operated at 2.8 to 3.0 bar, the Liquid Oxygen (LOX) tank at 1.97 to 2.06 bar. A spherical helium vessel for the pressurization of the pneumatic control system and the LOX tank is located at the bottom of the BMA carrying 172 l of GHe at 226 bar and 87 K

Each GTO mission is characterized by a mission profile that distinguishes between the On Ground Mission and the In Flight Mission. Both parts of a mission are characterized by a number of events and functions that need to be fulfilled by different components of the launcher. The flight phase again is separated into 4 sections of different boost phases:

- EAP/EPC thrust phase
- ESC-A thrust phase (HM7-B engine)
- ballistic phase
- stage passivation phase

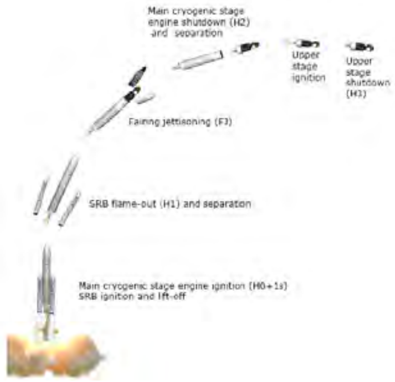

The ballistic phase (*or:* SCAR phase) represents the crucial phase for the present analysis. During the ballistic phase the upper composite is oriented by the SCAR system. This includes thermal control manoeuvres, sun-angle orientation manoeuvres, and providing spin to the payload. The ballistic phase is a prerequisite for the proper injection of the payload into its defined orbit.

The SCAR system (**S**ystème de **C**ontrôle d'**A**ttitude et de **R**oulis) is located at two positions: While the Outer SCAR (OSCAR) is located on the Elongated Lower Skirt (ELS) the Inner SCAR (ISCAR) is located directly at the inter-stage on the BMA. Both, OSCAR and ISCAR include 2 clusters positioned on opposite sides of the stage. The right Figure shows the OSCAR cluster located on the Z axis. Each cluster is equipped with 3 nozzles.

The function of the SCAR system is to control the roll of the stage during the HM7-B firing phase and to control roll, pitch and yaw during the ballistic phase. The SCAR system is propelled by gaseous hydrogen and fed through the engine's regenerative channel via the pressure regulator D46 during HM7-B firing and directly through the hydrogen's tank pressurization channel during the ballistic phase. Each line, divider and nozzle of the SCAR system with its unique physical characteristics is described.

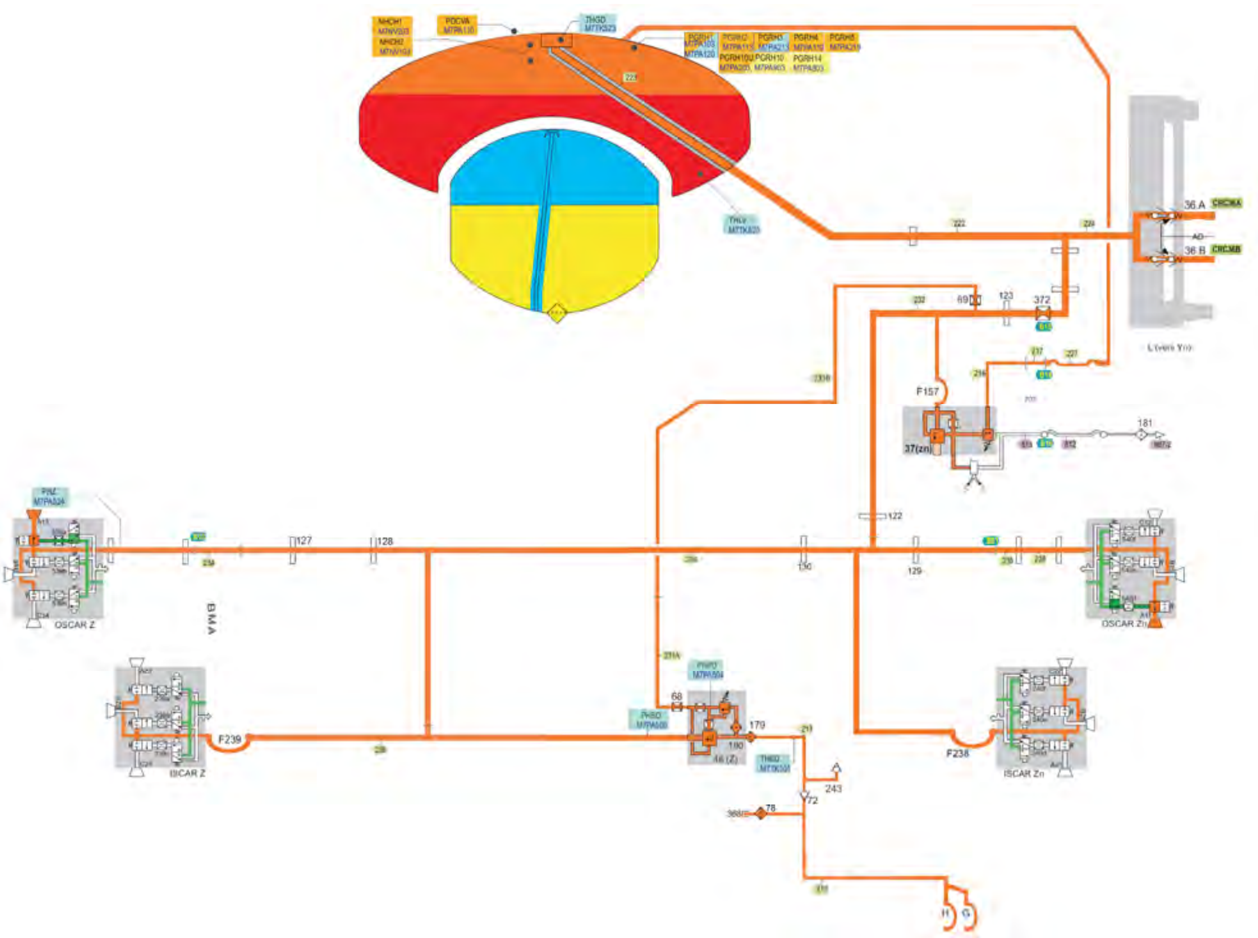

Figure III-1. GH2 SCAR Pressure Lines

Figure III-1 is an extract of the stage functional schematic and shows the pneumatic schematic of all GH2 pressurization lines of the SCAR system. In the following the position of each line is briefly described:

- Line 223 is the out-gassing line of the propellant GH2 and is located inside the LH2 tank.
- Line 222 connects the gas side of the LH2 tank to line 224.
- Line 224 connects the tank line 222 to BMA line 232.
- Line 232 connects the tank line 224 to the T junction of line 230.

- Lines 230, 234, and 235 are the distribution lines for any GH2 across the BMA for SCAR activation. In order to process the technical data in a way that it can be used as input data for the simulation, line 230 is divided into two parts, 230a and 230b, representing the part of line 230 starting at the intersection with line 232 (inlet) and going downstream towards the Zn and Z axis respectively. Line 234 ends at the interface to line 228.
- Lines 230b and 235 run from the T of BMA line 232 to line 229 and hence feed OSCAR and ISCAR on the Z axis.
- Line 228 connects BMA line 234 to OSCAR Zn coupling on the ELS.
- Line 229 connects BMA line 235 to the OSCAR Z coupling on the ELS.
- Line 238 connects BMA line 230 to ISCAR Zn.
- Lines 236 and 239 connect BMA line 230 at its divider D230 to the ISCAR Zn coupling.

Each SCAR thruster block is equipped with three nozzles, one vectoring the thrust outwards, i.e. parallel to the Z and Zn axis, and two delivering thrust in opposite directions and tangential to the circumference of the stage. Each block is divided into two functional parts which fulfil the following tasks:

1. The command part is equipped with 3 electronic pilot-controlled valves which can activate each nozzle independently. The valves are supplied with 23 ± 1 bar Helium from the command circuit.
2. The power section consists of 3 nozzles and valves which are activated by the command valves and enable the gaseous Hydrogen to enter the nozzles.

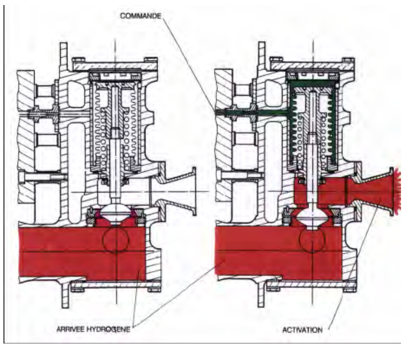

A more detailed view of the power section which represents the important part of the SCAR block can be seen in right figure showing the gaseous Hydrogen distribution in a SCAR block during non-activation and activation. The flow contraction coefficient, the velocity coefficient and the time constant of the valve are introduced along with the governing equations in section V.

The liquid Hydrogen tank is located at the top of the upper stage right below the A5 Vehicle Equipment Bay (VEB). Right Figure shows the main dimensions of the tank. The tank is divided into 4 sections. Each section is specified by its individual temperature and heat flux for the simulation case.

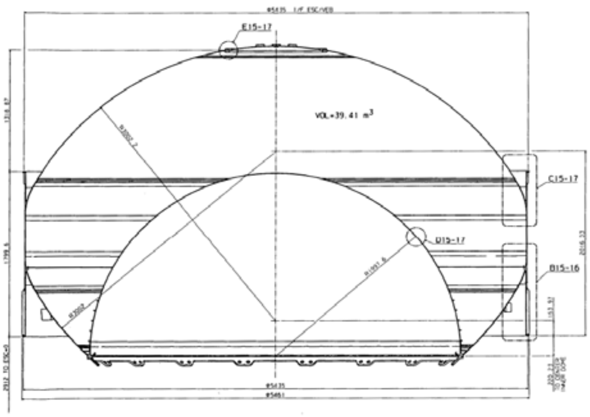

1. Upper Dome: The upper dome has an inner radius of 3002.2 mm and is made of Aluminium AL2219 with a thickness varying between 1.7 to 4 mm.
2. Cylinder: The cylinder is the centre part of the tank and located between the upper and lower dome with a diameter of 5410 mm.
3. Lower Dome: The lower dome connects the cylinder to the inner dome. The inner radius is 3002 mm. In settled mode the liquid Hydrogen is in contact with the lower and inner dome.
4. Inner Dome: The inner dome is the inner part of the LH2 tank. Its concave shape makes the geometrical layout possible with the LOX tank located in-between the LH2 tank. Its inner radius is 1997.6 mm.

Due to the very low boiling temperature of 20K for liquid Hydrogen, the entire insulation of the stage is carried out quite extensive. The insulation material is mainly Dacron which is a polyester fiber. The external surface of cylindrical part is covered Cryosof which a closed porous foam. The stage is vented with Helium during the launch preparation therefore also the Dacron insulation.

IV. ESC-A SCAR Phase Simulation Model

The S/W used to simulate the ESC-A SCAR system is EcosimPro kernel using euces COMPONENTs. In order to ensure the clarity and the right interpretation of results due to the change of parameters the correlation is subdivided into 3 steps:

1. Correlation of the nozzles
   This 1st step ensures that the nozzles give the correct results. This is an important prerequisite, because a wrong mass flow rate would result in deviating pressures, temperatures, evaporation rates and propellant mass. Therefore, the nozzles have to be verified before the simulation of the entire system.
2. Correlation of lines and divider
   The next step includes the verification of all lines and dividers which of course influence the entire system in terms of friction and pressure.
3. Correlation of the entire system including tank
   The true correlation of the entire system is performed as a last step. Knowing that a given pressure results in a correct mass flow rate gives the possible to determine the right diffusion rates and initial temperatures in the tank.

A. Nozzle Correlation

The 1st part of the correlation covers the SCAR nozzles. With a fairly simple set of equations the nozzles influence the entire pressure evolution in the SCAR system. Because each nozzle has the same physical characteristics it is not necessary to distinguish between them as it is necessary for lines.

The data for the SCAR nozzles is related to a single thruster:

- 56 N at gaseous Hydrogen injection with an inlet pressure of 2.85 bar and
- a temperature of 150 K. The specific impulse is ~180 s.

With the given specific impulse and thrust the according mass flow rate can be calculated to 31.78 g/s. Besides appropriate boundary conditions the following hardware parameters are given for the model:

- throat diameter: d_{th} = 13.8 mm
- nozzle diameter: d_n = 29.9 mm
- flow contraction coefficient: α_{noz} = 0.85
- velocity coefficient: φ_{noz} = 0.962

The results are shown below. They are complied the technical specification. For the pressure evolution inside the entire SCAR system the crucial value is the mass flow rate. The negligible deviation of 1.6% proves that the flow contraction coefficient α_{noz} has been chosen adequately. In order to adapt the computed values for the thrust and specific impulse, the velocity coefficient has adopted to φ_{noz} = 0.962. The calculation delivers:

Variable	Unit	Specification	Result
F	N	56.1	56.089
I_{sp}	s	~ 180	182.8
$\dot{m}$	g/s	~ 31.78	31.28

Table IV-1. Comparison between specified Values and Model

B. Lines Correlation

The following section of the model verification covers the whole SCAR system with all components *except* the propellant tank. The model built-up can be seen in Figure IV–1.

The model is used to simulate the pressure conditions inside the lines as a function of loss coefficients, mass flow rates, enthalpy flow rates, density, cross sectional areas and thrusters activation. The tank is not included and replaced by a boundary with time-dependent pressure and temperature measured inside the LH2 tank during the respective flight phase. As a reference for the pressure inside the SCAR system the only pressure transducer M7PA524 in the LH2 part is used. It is located at line 229 and measures the gas mixture's static pressure shortly behind the line's longest straight section and approximately 557.3 mm upstream the interface to the OSCAR Z block.

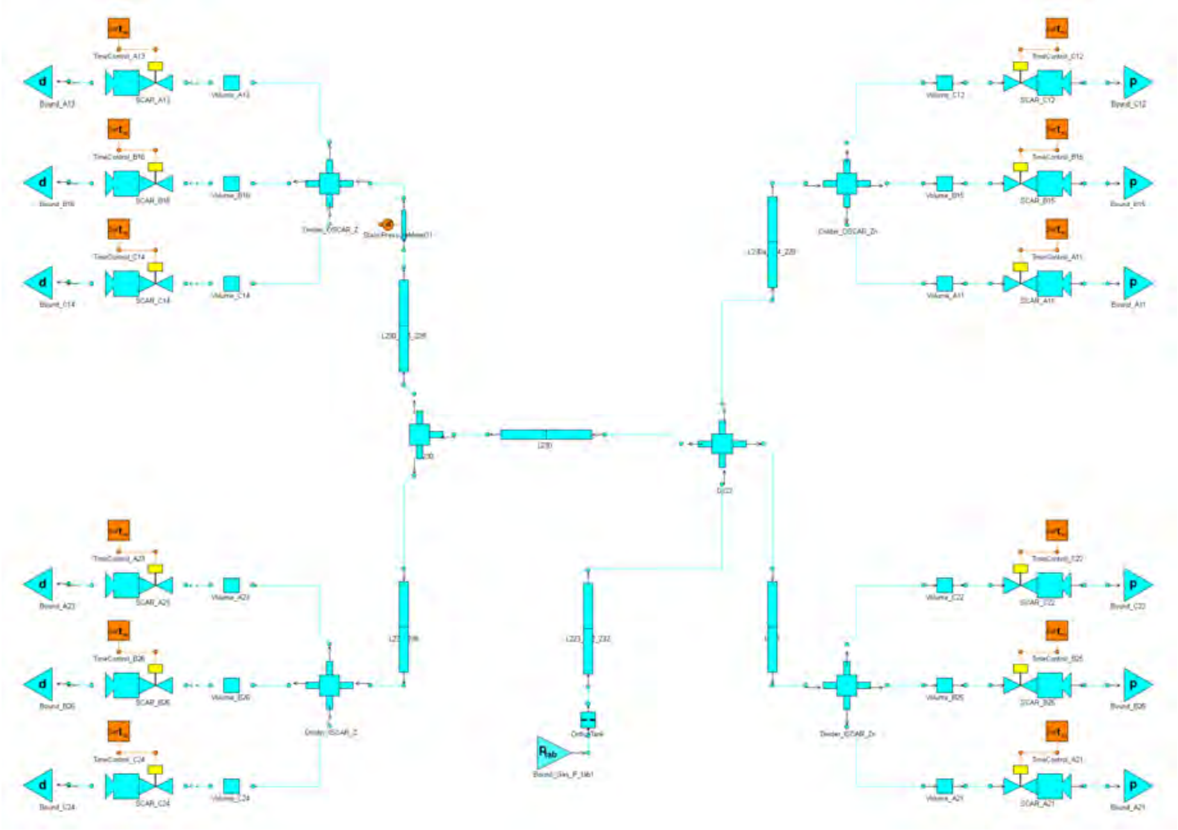

Figure IV-1. euces Model without Consideration of the Propellant Tank

Line	L [m]	d_i [mm]	ζ
L223	3.765	60	1.695
L222	0.166	64.4	9.663
L224	1.481	70	1.071
L232	0.874	70	3.797
L230a, 234	0.596	40	0.564
L230b, 235	2.713	40	1.772
L228	1.909	70	1.536
L229	1.909	70	1.536
L238	0.67	40	1.522
L236, 239	1.171	40	2.003

Table IV-1. Lines Data

For the correlation without the tank the boundary for the system inlet pressure is preset by the sensors M7PA103, M7PA113, M7PA203 and M7PA213 measurements as the time-dependent arithmetical mean, respectively. The temperature is preset by sensor M7TK523 measurement. Phases of measurements due to contact with liquid Hydrogen are not considered and linear interpolated between the last valid measurement and a reasonable recovery time aligning the linear approximation to the original curve.

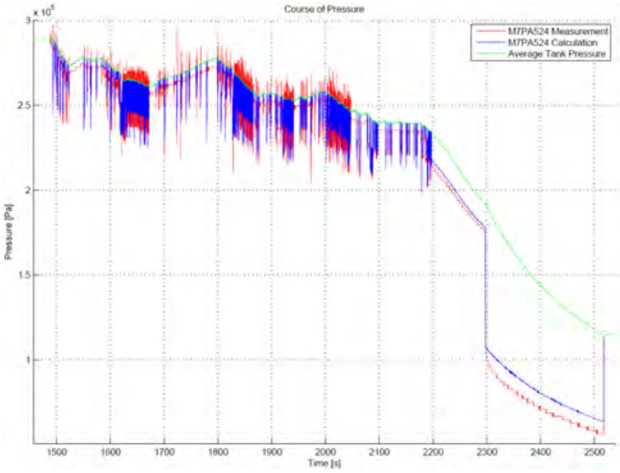

Figure IV-2. Simulation vs. Measurement of Sensor M7PA524

Figure IV–2 shows the result of the simulation for the line pressure. The comparison between the simulated values (blue curve) and the measurement (red curve) shows that the calculated pressure follows the slope of the measurement quite well which fulfils the expectations, because the measured tank pressure (green curve) has been used as input boundary. Therefore, the magnitude and slope of the 2 curves have to be similar. But, there exists also an offset between the simulation and the measurement. Obviously, this deviation results from an already existing offset between M7PA524 measurement and the average tank pressure which is the input boundary for the simulation. The fact that the simulation approaches the value of the tank pressure when no valve is opened confirms the assumption of different measurements being the reason for the offset.

However, a closer look at flight L522 calibration data provides a possible explanation. The crucial sensor M7PA524 (SCAR sensor) has the largest tolerance of 63 mbar. Under consideration of the tolerances of the tank sensors a maximum deviation of 79 mbar is possible, assuming that all tank sensors are providing their maximum deviated values and the SCAR sensor gives its lowest deviated value.

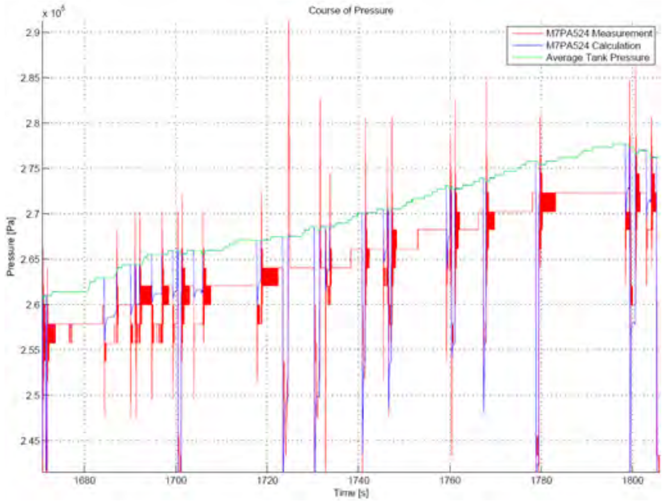

Figure IV-3. Offset between M7PA524 Measurements and the average Tank Pressure

This of course has a low probability to happen, but has to be considered. Therefore, the deviation between the SCAR sensor and the tank sensors' average is within the tolerance as seen in Figure IV–2, which shows a maximum deviation of 50 to 60 mbar. The offset between simulated and measurement values is therefore also within the tolerance.

Besides the offset, it is also obvious that the measurement shows quite an overshot and oscillation whenever a valve closes as shown in Figure IV–3. This is the reason why the measurement seems to be located highly above the simulation over extensive time periods in Figure IV–2. The oscillation is due to the fact that the sensor is connected via a thin line to line 229 rather than being directly flash-mounted. It is obvious that a long and thin transducer line may be responsible for the oscillation but definitely plays an important role for it.

C. System Correlation

In the final part of the correlation the tank is added to the model which is shown in Figure IV-4. The tank model includes all phenomena regarding heat transfer through walls, liquid and vapour part as well as heat and mass transfer between liquid and vapour phase interface. The procedure of the correlation covers 2 steps:

- In a 1st step the system is modelled according to the specific case. The goal is to analyze the system with respect to varying input parameters and thermal variables. The influence of different assumptions was analysed and their effect on the simulation results.
- Secondly the hot and cold case simulations for flight L522 were computed. The specific case in the 1st step has been set between the hot and cold case.

Flight measurements serve as the basis for the evaluation of the computed values. Since the present correlation is focused on the tank, the regarded sensors include the LH2 pressure sensors M7PA103, M7PA113, M7PA203 and M7PA213 as well as the tank's liquid and ullage temperature sensors M7TK522 and M7TK523.

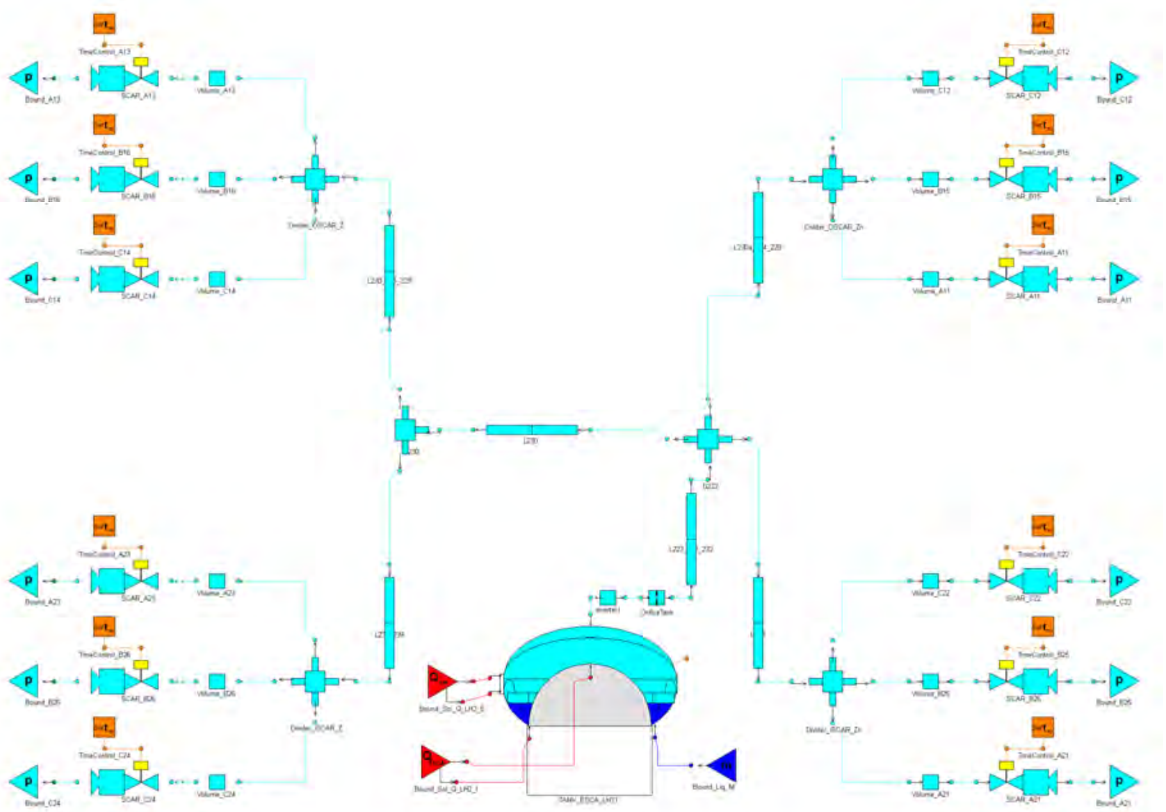

Figure IV-4. euces Model with Consideration of the Tank

The pressure sensors are located at the top of the LH2 tank next to the gas diffuser. In order to be able to compare the computed results to accurate measurements the mean value of the four mentioned sensors is used which is denoted as the *Average Tank Pressure* in all diagrams displaying the pressure evolution.

The two temperature sensors inside the LH2 tank are M7TK523 and M7TK522. M7TK523 is located at the very top of the tank inside the diffuser. Measurements show that sensor M7TK523 occasionally has contact to liquid Hydrogen which of course leads to unusable results. The same incidents can be seen on the M7TK522 measurements. At times the sensor is out of measurement range, because it is in contact with the gaseous Hydrogen.

The input values for the simulation contain all assumptions made in previous chapter which includes the SCAR thruster activation sequence, the tank pressure, the liquid temperature, the distribution of ullage temperatures and wall temperatures. Additionally, *constant* heat and mass transfer coefficients are applied, i.e. the control flags M_flag and Q_flag within the init data wizard were still set to FALSE.

Taking a closer look at the obtained results leads to the following observations:

- Pressure Gradients and Offset
  a. The simulated slope of the pressure follows the measurement precisely enough considering that the results are obtained from a numerical simulation with residual propellant in settled position. Deviations occur at various events in the simulated phase. Directly at the beginning the pressure gradient is too high, leading to a deviation of 0.116 bar at t =1550 s, which corresponds to a relative error of 4.16 %. After approximately 1400 s the simulation follows the measurement very closely. From 2110 s onwards the pressure again develops too high. As soon as the mass flow reaches its maximum the exact opposite occurs leading to the simulation's maximum (negative) deviation at the end of the simulation after the passivation phase at t =2519 s which is −0.137 bar or −12 %.

  b. Shortly before 1600 s the two curves start approaching each other. The slope of the simulated curve is constantly below the measured one leading to small deviations of only 0.023 bar at 1800 s.

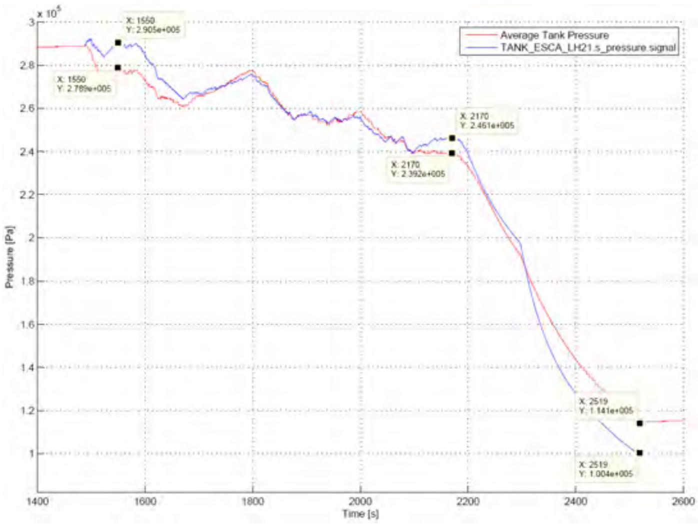

Figure IV-5. Pressure Evolution of Simulation 1

- Liquid Temperature
  a. Regarding the temperature evolution in Figure IV-6 the before mentioned effect of degraded measurements becomes clear. Propellant sloshing inside the LH2 tank leads to a distribution on the liquid hydrogen in such a way that the gaseous Hydrogen interferes with the M7TK522 measurement.

  b. A constant offset between the calculated and the measured liquid Hydrogen temperature is present.

  c. The measured liquid temperature in Figure IV-6 starts at 23 K, increases at approximately 1615 s from shortly above 23 K to an average of 23.5 to 24 K before it finally starts to decrease with the beginning of the spin-up phase of the stage. In contrast, the simulated temperature remains rather constant. Over an interval of 700 s it decreases quite steadily from 24.374 K to 2.83 K.

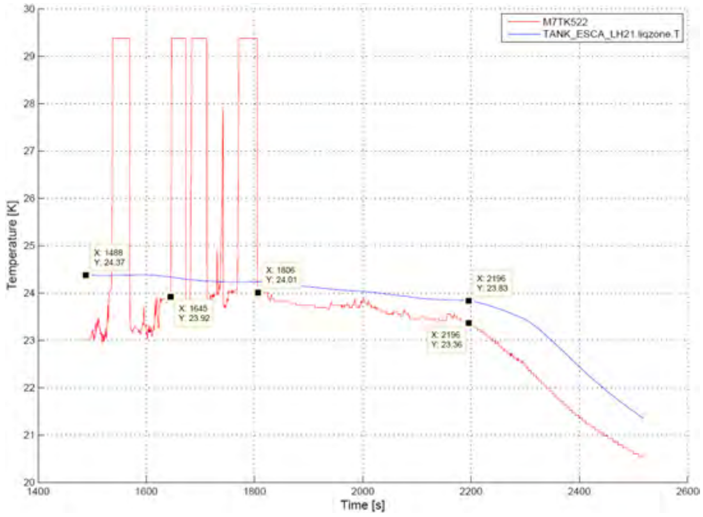

Figure IV-6. Liquid Temperature Evolution of Simulation

- Ullage Temperature
  a. The measurement of the ullage temperature in Figure IV-7 shows the expected behaviour of phases before sloshing of liquid hydrogen occurs. The overall slope shows exponential decay.
  b. The overall slope of the simulated ullage temperature follows the measurement in the 1st third of the simulation quite well. At approximately 1684 s the calculated value approaches a constant value while the measurement decreases further. From that point onwards the deviation remains with average 20 K rather high.

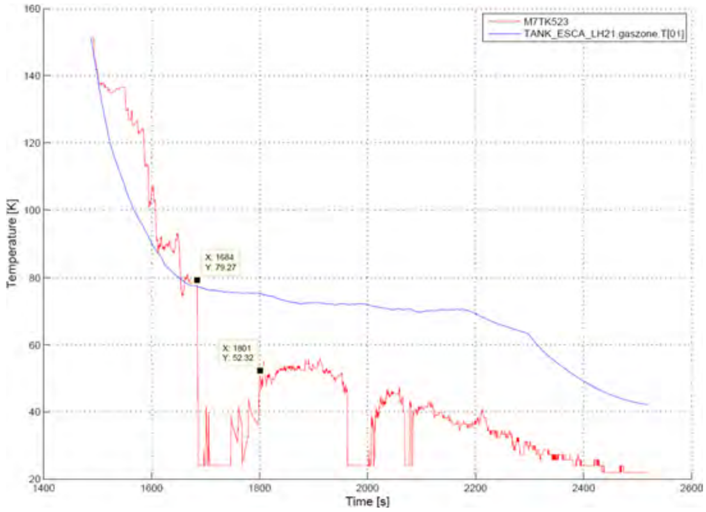

Figure IV-7. Ullage Temperature Evolution of Simulation 1

- Occurrences of "limit range" Measurements
  The periods of the ullage sensor M7TK523 and the liquid sensor M7TK522 being out of range are overlapping but not identical. The liquid sensor's disturbances start and end earlier than the ones registered during the ullage measurements. However, shortly before *Spaceway-2* satellite separation both sensors start giving "limit range" data just about simultaneously. While the ullage temperature is out of range between 1685 s and 1801 s the liquid sensor is influenced between 1645 s and 1806 s after H0.

- Pressure Gradients and Offset
  Liquid Temperature
  One possibility for the too high pressure development at the initial phase of the simulation could be a too high liquid temperature. The saturation temperature of 24.374 K has been used as the initial temperature. Because the overall pressure evolution fits the measurement well this seems to be a reasonable assumption, however M7TK522 measurements, as seen in Figure IV-6, show that the true ullage temperature is more than 1 K below this assumption. It is realistic to take the liquid in settled mode as a starting point. With the initial propellant mass of 331 kg the liquid level at the beginning of the simulations is ~0.849 m. Sensor M7TK522 is located at 0.732 m. Heat loads from the ullage are effecting the liquid's surface, the warmer liquid hydrogen stays in the upper layer stratified and no natural reorientation occurs. This leads to a linear temperature distribution through the liquid. Because the surface temperature is the saturation temperature all layers below have to have a lower temperature. This could be the reason for the temperature to be assumed too high, providing a higher overall energy to the system and resulting in more evaporation at the beginning. In fact the M7TK522 measurement in Figure IV-6 confirms this possibility of an uneven temperature distribution. After the liquid has been mixed the average temperature remains at steady state between 23.4 and 23.8 K.

- Sloshing
  The most extensive simplification of the tank model is the modelling of settled propellant condition during ballistic phase. In reality sloshing of the liquid Hydrogen occurs at all times as already noticed in ullage and liquid temperature measurements. Sloshing influences the thermal conditions in the tank in 3 ways:

  1. The arbitrary distributed liquid results in a much greater interface area between the two phases vapour and liquid. According to theory the contact area has a linear influence on the evaporated mass. After all this fact leads to a higher tank pressure.
  2. Also the increased interface area assists a better heat exchange between ullage and liquid, leading to a higher liquid temperature and lower ullage temperatures.
  3. When sloshing is apparent the liquid is not only in contact with the cold bottom of the tank, but also in contact to warmer parts of the tank. Especially in the upper regions, the liquid heats up which results in higher temperature and evaporated mass as well. Both processes are neglected in the simulation, but their effects can be seen in the obtained pressure results. Between 1684 s and 1801 s both temperature sensors (M7TK522 and M7TK523) were affected by sloshing. At the same time, the simulated evaporation in figure Figure IV-5 develops too low. After 1870 s the slope of pressure is parallel to the measurement which corresponds to the results presented in [8].

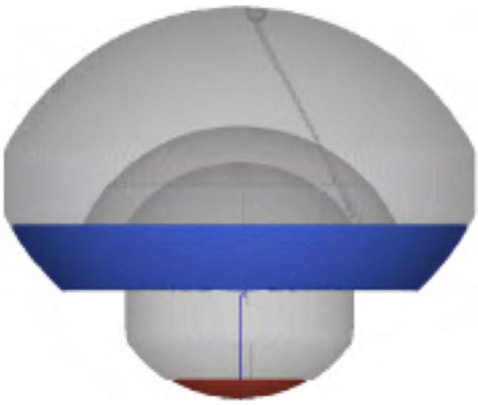

(a) Settled Propellant Condition, *t* = 1488 s

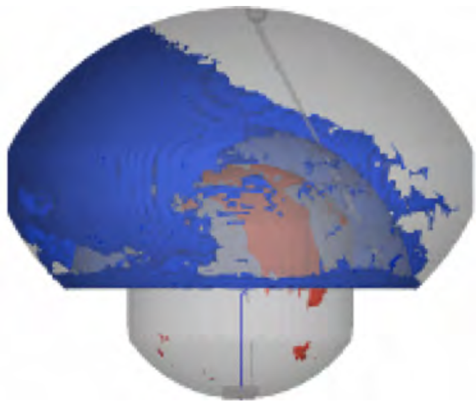

(b) Sloshing, *t* = 1637 s

Figure IV-8. Example for Sloshing during the SCAR Phase [8]

V. Conclusion

With the performed correlations one comes to the following 3 observations:

- The obtained results for the nozzle correspond well to the specification of the nozzles.
- The pressure evolution during the simulation without the tank is within the tolerance of sensor M7TK524 even during phases of high mass flow rates.
- The tank correlation delivers for most parts realistic results provided that the adaptable hardware parameters are set accordingly. However, a too high evaporation at the beginning of the simulation influences the first 200 s of the simulation noticeable.

After the ESC-A SCAR phase correlation of L522 it can be concluded that even though the tank model with settled propellant is a crucial simplification with respect to the phase interface contact area between liquid and ullage coupled with liquid sloshing which results in additionally transferred heat, it still delivers very realistic results.

Acknowledgments

The **euces** project Part II was funded by BMBF (federal ministry of education and science) with account no. 50RL0620 and was performed at EDAS Astrium GmbH.

References

Reports, Theses, and Individual Papers

[1]Isselhorst, A., ***euces**: **eu**ropean **c**ryogenic **e**ngineering **s**oftware tool*, AIAA 2006-6729, AIAA Modelling and Simulation Technologies Conference and Exhibit, 21-24 August 2006, Keystone, Colorado

[2]Isselhorst, A, Rackemann N., ***euces** Software Development*, ICES 2008-01-2072, 38th International Conference on Environmental Systems, San Francisco, California June 30 - July 3, 2008

[3]Isselhorst, A.; ***euces,** Simulation of Launcher Propulsion Systems, Study on numerical Modeling and Simulation of Launcher Stages for propelled and non-propelled Flight Phases*, Final Report Part I, EADS-ST **euces**-RIBRE-FR-0001, 2006.

[4]Isselhorst, A.; ***euces,** Simulation of Launcher Propulsion Systems, Object-oriented Programming of physical Models for Launcher Propulsion Systems*, Final Report Part II, EADS-ST **euces**-RIBRE-FR-0002, 2008.

[5]Bergemann, K., *Execution of ESC-A ballistic Phase Simulations with **euces** EcosimPro Model*, Diploma Thesis, University of Applied Sciences Oldenburg/Ostfriesland/Wilhelmshaven, Sep. 2008

Computer Software

[6]EcosimPro; *A Professional Dynamic Modeling and Simulation Tool for Industrial Applications*, Ver. 3.4.2, EAI **E**mpresarios **A**grupados **I**nternational, Madrid, Spain, 2006.

EADS-ST Internal Documents

[7]Kleinert-Alvarado, G.: *Hydraulic Configuration of ESC-A*, EADS Astrium GmbH, Germany, A5-NT-13-A-0074-DASA, Iss. 4, Rev. 1 (2002)

[8]Michaelis, M., *V522 Niveau 1 Evaluation: Study of ESC-A Propellant Sloshing during SCAR and Passivation Phase w.r.t. cinematic Behaviour during Passivation Phase*, Astrium GmbH, Bremen, Germany, A5-NT-133-A-0018-DASA, Iss. 1 (2006)